FULL PAPER

Dalton
www.rsc.org/dalton

Solid-state spectroscopic properties and the geometry of binuclear rhodium(I) diisocyanoalkane complexes†

Oksana Gerlits, Andrey Yu. Kovalevsky and Philip Coppens*

Chemistry Department, University at Buffalo, State University of New York, Buffalo, NY 14260, USA. E-mail: coppens@buffalo.edu

Received 24th August 2004, Accepted 7th October 2004
First published as an Advance Article on the web 27th October 2004

A series of crystalline dinuclear rhodium complexes with different bridging diisocyano ligands and different counter ions have been studied by low-temperature crystallographic and solid-state spectroscopic techniques. The Rh–Rh distances vary from 4.5153(3) to 3.0988(7) Å, and the twist angles around the Rh–Rh line from 58.3(1) to 0°, both depending on the size and conformational rigidity of the bridging ligand. For very long distances as occur in the $[Rh_2(dimen)_4]^{2+}$ salts the absorption is significantly blue-shifted compared to other complexes. For a given cation a shorter Rh–Rh bond gives a red shift of the phosphorescence emission band, indicating a smaller energy gap between the ground and emitting excited states. An exception occurs for the $[Rh_2(1,6\text{-diisocyanohexane})_4]^{2+}$ ion, in which dimer formation in the calixarate salt lengthens the Rh–Rh intramolecular bond length without affecting the emission spectrum.

Introduction

Since the first synthesis of $[Rh_2(diprop)_4]^{2+}$ (diprop = 1,3-diisocyanopropane) in 1976 by Gray *et al.*,[1] and its proposed use for hydrogen gas production in solar energy conversion schemes,[2,3] the photochemistry and photophysics of the binuclear Rh(I) and related complexes have been studied extensively,[4] and several room-temperature crystal structures have been reported.[5–7] On excitation highly reactive phosphorescent triplet states are formed with lifetimes of the order of μs.

Though such transient species are of crucial importance as intermediates in chemical reactions, diffraction information on the structures of these species has not been available. However, recent progress in time-resolved (TR) diffraction techniques is opening up this field.[8,9] d^8–d^8 binuclear Rh complexes are excellent candidates for TR diffraction studies as according to spectroscopic analysis and theoretical calculations they show pronounced shortening upon excitation.

We have recently reported the first TR diffraction study of a dirhodium complex.[10] For the time-resolved results to be placed in proper context, information on the structure and solid-state spectroscopic properties of the class of compounds being studied is essential. We report here very low temperature (18–20 K) solid-state emission spectra, room-temperature absorption spectra and 90 K crystal structures of a series of binuclear dirhodium solids with the bridging ligands diprop (= 1,3-diisocyanopropane), dihex (= 1,6-diisocyanohexane) and dimen (= 1,8-diisocyano-*p*-menthane). This is the first report on the synthesis, spectroscopic and structural studies of the complexes containing the $[Rh_2(dihex)_4]^{2+}$ cation. Various counterions, including $[PF_6]^-$, $[BPh_4]^-$ and [calix[4]arene − H]$^-$, were used, the latter to reduce the cation concentration in the solid state,[11] so that in the TR diffraction experiments fewer photons will be required to excite a specific fraction of the photoactive species. The results are compared with our theoretical study on the $[Rh_2(diprop)_4]^{2+}$ ion.[12]

Experimental

Preparation of the dinuclear rhodium(I) complexes

Starting materials. $[Rh(COD)Cl]_2$ (COD = 1,4-cyclooctadiene), 1,6-diisocyanohexane (dihex), $AgPF_6$ and $NaBPh_4$ were obtained from Aldrich and used without further purification. 1,3-Diisocyanopropane and 1,8-diisocyano-*p*-menthane were prepared from the corresponding amines as described in the literature.[13] Tetramethylammonium calix[4]arenate (TMACalix) was synthesized by the method of Harrowfield *et al.*[14] $[Rh_2(diprop)_4]Cl_2$ was prepared as described in the literature.[15b]

$[Rh_2(diprop)_4][BPh_4]_2$ (1), $[Rh_2(diprop)_4][BPh_4]_2\cdot CH_3CN$ (2), $[Rh_2(diprop)_4][BPh_4]_2\cdot 1.6C_6H_5CN\cdot 0.4C_6H_5Cl$ (3). The $[Rh_2(diprop)_4][BPh_4]_2$ complex was prepared by a known procedure.[15b] Crystals of **1** were obtained by slow evaporation of benzonitrile solution, while crystals of **2** were prepared by diethyl ether vapor diffusion into an acetonitrile solution of the dirhodium complex. Crystals of **3** were grown by slow evaporation of a $[Rh_2(diprop)_4][BPh_4]_2$ solution in a mixture of benzonitrile and chlorobenzene.

$[Rh_2(diprop)_4][Calix]_2$ (4). A mixture of two solids, TMACalix (0.076 g, 0.153 mmol) and $[Rh_2(diprop)_4]Cl_2$ (0.05 g, 0.0765 mmol), in stoichiometric amounts was completely dissolved in methanol (≈50–60 ml). During mixing and gentle heating a precipitate started to form. The product $[Rh_2(diprop)_4](Calix)_2$ was obtained as a dark blue, very fine, solid. Crystals of **4** were grown by diethyl ether vapor diffusion into a solution of the complex in acetonitrile.

$[Rh_2(dihex)_4][PF_6]_2$ (5). $[Rh_2(dihex)_4][PF_6]_2$ was synthesized as reported in the literature for similar compounds.[7] $AgPF_6$ (0.051 g, 0.2 mmol) was added to a stirred solution of $[Rh(COD)Cl]_2$ (0.05 g, 0.1 mmol) in acetonitrile (5 mL). The resulting blend was mixed for 15 min after which a AgCl precipitate was removed by filtration. 1,6-Diisocyanohexane (0.067 mL, 0.4 mmol) dissolved in 1–2 mL of acetonitrile was then added to the yellow filtrate upon which the solution turned dark maroon. Diethyl ether was added to precipitate the product. Yields were in general poor (≈20–30% based on $[Rh(COD)Cl]_2$) and variable. Crystals of **5** were prepared by diethyl ether vapor diffusion into a solution of the dirhodium complex in an acetonitrile and methylene chloride mixture.

$[Rh_2(dihex)_4][Calix]_2\cdot 0.5C_2H_5OH$ (6). $[Rh_2(dihex)_4][Calix]_2$ was synthesized by adapting the procedure used for **5**. In the last step the reaction mixture was left to evaporate slowly, instead of precipitating the product by diethyl ether diffusion. A green-blue crystalline aggregate formed during a period of several days. Crystals of **6** were grown by diethyl ether diffusion

† Electronic supplementary information (ESI) available: A discussion on the disorder treatment; tables of crystallographic information. See http://www.rsc.org/suppdata/dt/b4/b412942c/

DOI: 10.1039/b412942c

into a solution of the complex in a mixture of methylene chloride and dimethyl sulfoxide.

$[Rh_2(dimen)_4][PF_6]_2 \cdot CH_3CN$ (7). $[Rh_2(dimen)_4][PF_6]_2$ was prepared as described in the literature.[16] Crystals of **7** were obtained by diethyl ether vapor diffusion into an acetonitrile solution of the compound.

$[Rh_2(dimen)_4][Calix]_2 \cdot 0.64H_2O$ (8). $[Rh_2(dimen)_4][Calix]_2$ was prepared similarly to **7**. During the last step of the synthesis a methanolic solution of TMACalix was added to a solution of the dirhodium complex in methanol. After mixing the resulting solution became cloudy. The mixture was left to evaporate slowly, crystals of **8** formed overnight.

X-Ray crystallography

X-Ray diffraction data on **1–5**, **7** and **8** were collected at 90(1) K using a Bruker SMART1000 CCD diffractometer installed at a rotating anode X-ray source (Mo-Kα radiation), and equipped with an Oxford Cryosystems nitrogen gas-flow apparatus. The data were collected by the rotation method with 0.3° frame-width (ω scan) and 10–60 s exposure time per frame. For each complex four data sets (600 frames in each set) were collected, nominally covering half of reciprocal space. The data for **6** were collected at 16 K on the X3 beamline at the National Synchrotron Light Source at Brookhaven National Laboratory. The data were integrated, scaled, sorted and averaged using the SMART software package.[17] The structures were solved by direct or Patterson methods, using SHELXTL NT Version 5.10[18] and refined by full-matrix least squares against F^2. The displacement parameters of the non-hydrogen atoms were refined anisotropically. Positions of hydrogen atoms were found from difference Fourier maps and refined using a "riding" model with fixed $U_{iso} = 1.2U_{eq}$ of the attached carbon atom ($U_{iso} = 1.5U_{eq}$ for CH_3, OH and H_2O hydrogen atoms).

In several cases geometry restraints were applied. Details on the restraints and the treatment of the disorder are given in the ESI.† Crystallographic data for complexes **1–8** are presented in Table 1. Final positional, isotropic and anisotropic displacement parameters together with full list of bond lengths and angles are given in Tables S1–S24 of the ESI.†

UV-Vis reflectance and photoluminescence spectroscopy

UV-vis absorption experiments were performed on a Perkin-Elmer Lambda 35 UV-Vis spectrometer equipped with an integrating sphere for diffuse reflectance spectroscopy. The spectra were collected in the 300–1100 nm range at room temperature. Powdered crystals homogeneously diluted with a non-absorbing matrix (MgO) and gently tapped into a sample holder were used as samples.

Photoluminescence measurements were carried out on a home-assembled emission detection system. Samples (several small single crystals) were mounted on a copper pin attached to a DISPLEX cryorefrigerator. A metallic vacuum chamber with quartz windows is attached to the cryostat, the chamber was evacuated to approximately 10^{-7} bar with a turbo-molecular pump, which allows cooling down to 17–18 K. The crystals were irradiated with 440 or 500 nm light from a pulsed N_2-dye laser. The emitted light was collected by an Oriel 77348 PMT device, positioned at 90° to the incident laser beam, and processed by a LeCroy Digital Oscilloscope with 1–4 GHz sampling rate.

Results and discussion

Conformation of the $[Rh_2(diprop)_4]^{2+}$, $[Rh_2(dihex)_4]^{2+}$ and $[Rh_2(dimen)_4]^{2+}$ cations

The $[Rh_2(diprop)_4]^{2+}$ cations in **1–3** adopt similarly eclipsed conformations of the paddle-wheel structure in all solids studied (Fig. 1), while the geometry of **4** is slightly twisted. In **1–4** the

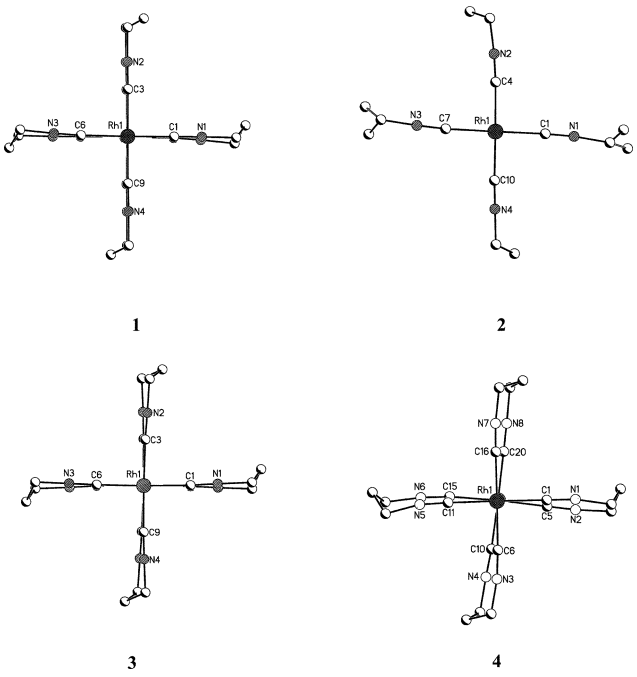

Fig. 1 Geometries of the $[Rh_2(diprop)_4]^{2+}$ cation in complexes **1** ($[BPh_4]^-$), **2** ($[BPh_4]^- \cdot 1.0CH_3CN$), **3** ($[BPh_4]^- \cdot 1.6C_6H_5CN \cdot 0.4C_6H_5Cl$) and **4** (calix[4]arenate), viewed along the Rh–Rh axis.

Rh–Rh distance varies by not more than a few hundredths of an Angstrom (3.296(1) Å in **1**, 3.2222(5) Å in **2**, 3.2397(6) Å in **3** and 3.2262(5) Å in **4**).

In **1–3** each Rh atom has an almost perfect square-planar configuration. The distortions do not exceed 3°. Projections along the Rh–Rh axis of **1** and **3** show the central CH_2 groups of the propyl bridge bent either towards and away from the CH_2 group in the adjacent ligand (Fig. 1). For **2** the disorder of the CH_2 groups indicates a superposition of different conformers in an 80–20% ratio.

In the calix[4]arenate salt **4**, the orientation of the methylene groups of the propyl bridges in the $[Rh_2(diprop)_4]^{2+}$ cation is intermediate between those observed for **1–3** (Fig. 1). Each Rh atom in **4** shows a small tetrahedral distortion with two *trans* carbons of the RhC_4 unit being displaced towards (the bond angles C1–Rh1–C11 and C10–Rh2–C20 are 174.1(2) and 174.7(2)°, respectively) and the other two pointing away (C6–Rh1–C16 and C5–Rh2–C15 are 178.5(2) and 176.4(2)°, respectively) from the center of the cation.

According to the DFT calculations,[12] the potential energy surface of the $[Rh_2(diprop)_4]^{2+}$ cation shows two minima with conformations that differ in the (N≡)C–Rh–Rh–C(≡N) torsion (twist) angle, the eclipsed (with a twist of 2°) conformation being 1.0 eV (96.5 kJ mol^{-1}) lower in energy than the twisted conformation in which the twist angle equals 27°. The higher energy conformer does not occur in the series studied here, the largest twist angles being 6.4(2), 8.0(2), 8.1(2) and 8.5(2)° in **4**.

In the dihex complexes **5** and **6** the Rh–Rh distances are shorter, at 3.0988(7) Å in **5** and 3.207(2) Å in **6**. The conformation of the $[Rh_2(dihex)_4]^{2+}$ cations is markedly different from that of **1–4** (Fig. 2). The increased flexibility of the much longer carbon chain of the dihex ligand results in the isocyanide groups adopting a *gauche*-like conformation with (N≡)C–Rh–Rh–C(≡N) torsion angles of 53.6(2)° for **5** and 58.3(1), 55.8(2), 55.7(1) and 56.1(1)° for **6**.

In the dimen complexes **7** and **8** the Rh–Rh distances are 4.5153(3) and 4.033(1) Å, respectively. For such longer bonds the ligand twisting is minimal (Table 2). In comparison, $M_2(dimen)_4$ (M = Rh, Ir) complexes with M–M distances less than ≈3.9 Å show a significant twist of the dimen ligands around the M–M axis.[5] For example, the $Rh(CN)_4$ units in $[Rh_2(dimen)_4][TFPB]_2$

Table 1 Crystallographic data for $Rh_2(diisocyanoalkane)_4^{2+}$ complexes

Cation	$[Rh_2(diprop)_4]^{2+}$	$[Rh_2(diprop)_4]^{2+}$	$[Rh_2(diprop)_4]^{2+}$	$[Rh_2(diprop)_4]^{2+}$	$[Rh_2(dihex)_4]^{2+}$	$[Rh_2(dihex)_4]^{2+}$	$[Rh_2(dimen)_4]^{2+}$	$[Rh_2(dimen)_4]^{2+}$
Counterion ·solvent	$[BPh_4]^-$	$[BPh_4]^-\cdot CH_3CN$	$[BPh_4]^-\cdot 1.6C_6H_5CN$ $0.4C_6H_5Cl$	[Calix[4]arenate]$^-$	$[PF_6]^-$	[Calix[4]-arenate]$^-\cdot$ $0.5C_2H_5OH$	$[PF_6]^-\cdot CH_3CN$	[Calix[4]arenate]$^-\cdot$ $0.64H_2O$
Compound	**1**	**2**	**3**	**4**	**5**	**6**	**7**	**8**
Empirical formula	$C_{68}H_{63}B_2N_8Rh_2$	$C_{70}H_{67}B_2N_9Rh_2$	$C_{74}H_{86}B_2Cl_2N_8Rh_2$	$C_{76}H_{67}N_8O_8Rh_2$	$C_{32}H_{48}F_{12}N_8P_2Rh_2$	$C_{89}H_{97}N_8O_{8.50}Rh_2$	$C_{50}H_{75}F_{12}N_9P_2Rh_2$	$C_{104}H_{118}N_8O_{8.64}Rh_2$
Crystal size/mm	0.15 × 0.15 × 0.025	0.33 × 0.05 × 0.03	0.40 × 0.17 × 0.03	0.30 × 0.15 × 0.05	0.15 × 0.15 × 0.08	0.10 × 0.01 × 0.01	0.10 × 0.08 × 0.03	0.25 × 0.13 × 0.05
Crystal system	Triclinic	Monoclinic	Triclinic	Monoclinic	Tetragonal	Tetragonal	Triclinic	Monoclinic
Space group	$P\bar{1}$	$P2_1/m$	$P\bar{1}$	$P2_1/c$	$P4_2/mnc$	$P4_32_12$	$P\bar{1}$	$P2_1/n$
a/Å	9.1489(5)	15.4675(5)	9.6380(2)	13.491(1)	13.0139(1)	19.02(1)	9.4476(2)	10.8626(3)
b/Å	12.5958(6)	12.4293(4)	12.7472(3)	27.858(2)	13.0139(1)	19.02(1)	13.4410(3)	30.3323(9)
c/Å	13.6740(7)	17.1086(5)	15.6755(4)	18.182(1)	26.2806(4)	45.85(2)	13.6704(3)	14.8705(5)
α/°	70.101(2)	90.00	67.898(1)	90.00	90.00	90.00	61.918(1)	90.00
β/°	76.012(2)	112.863(1)	74.235(1)	107.975(2)	90.00	90.00	84.857(1)	110.186(1)
γ/°	83.023(2)	90.00	84.374(1)	90.00	90.00	90.00	75.236(1)	90.00
V/Å^3	1436.4(1)	3030.7(2)	1717.20(7)	6499.8(9)	4450.93(8)	16589(16)	1480.07(6)	4598.7(2)
Z	1	2	1	4	4	8	1	2
D_c/g cm^{-3}	1.410	1.383	1.384	1.457	1.553	1.298	1.456	1.317
θ_{max}/°	22.52	28.30	23.26	25.01	30.02	20.00	30.05	25.12
Reflections collected	11477	49427	8763	54848	73815	53255	25586	53652
Unique reflections (R_{int})	3755 (0.0515)	7860 (0.0806)	4845 (0.0199)	10921 (0.0536)	3315 (0.0611)	10477 (0.0909)	8482 (0.0370)	8106 (0.0930)
Obsd. reflns. (no. params.)	2941 (240)	5461 (407)	4473 (389)	7360 (990)	2236	9226 (940)	7266 (394)	5482 (589)
R_1 ($F > 4\sigma(F)$), wR_2	0.0547, 0.1301	0.0391, 0.0994	0.0369, 0.1115	0.0551, 0.1617	0.0421, 0.1290	0.0787, 0.1911	0.0342, 0.0872	0.0724, 0.1649
Goodness of fit	1.038	1.025	1.099	1.060	1.155	1.224	1.046	1.099

Diprop = 1,3-diisocyanopropane; dihex = 1,6-diisocyanohexane; dimen = 1,8-diisocyano-*p*-menthane.

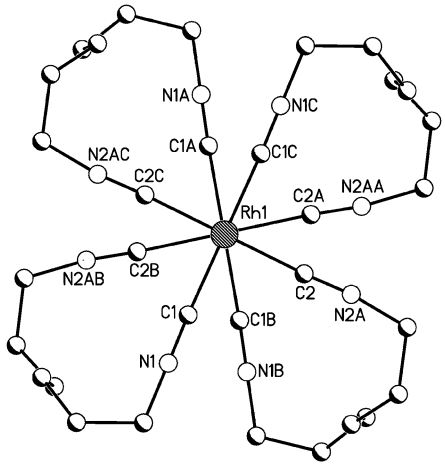

Fig. 2 Geometry of the $[Rh_2(dihex)_4]^{2+}$ cation in **5** (hexafluorophosphate), viewed along the Rh–Rh axis. The conformation of the $[Rh_2(dihex)_4]^{2+}$ cation in **6** is similar.

(tetrakis[3,5-bis(trifluoromethyl)phenyl]borate) (Rh–Rh = 4.25 Å) are eclipsed, whereas the average dihedral twist angle in $[Rh_2(dimen)_4][BPh_4]_2$ (Rh–Rh = 3.861 Å) is 16.2°.

The longer Rh–Rh distances of the dimen salts **7** and **8** and the smaller twist angles may be attributed to the rigidity of the cyclohexyl bridge of the dimen ligand. The geometry around the Rh atom in **7** is close to square-planar, with deviations not exceeding 4°, while in **8** Rh is shifted by 0.06 Å from the plane of the carbon atoms to the center of the cation, leading to a shorter Rh–Rh distance.

The correlation between the twist angle and intermetal distance in the Rh_2 complexes, with shorter distances generally corresponding to larger twist angles, is in agreement with the trend discussed in the literature.[5,12] The diprop compounds discussed above are exceptions, as a short distance occurs with an eclipsed conformation. The phenomenon that two otherwise identical complexes differ only in M–M distance and ligand twist angle has been described as 'deformational isomerism'.[5]

Intermolecular Rh–Rh interactions

While the dirhodium cations are generally monomeric, there is one exception (**6**) among the complexes studied. In the crystals, cations of **1** and **3** form columns of translation-related molecules along the crystallographic *a* axis (Fig. 3), with the Rh–Rh axis inclined by 38.8 and 10.8° to this axis in **1** and **3**, respectively. In **2** similar columns are formed along *b*, with an angle of 0° (Fig. 3). The distances between the Rh atoms of neighboring molecules are always more than 6 Å, which indicates the absence of a significant direct interaction. In **4** each $[Rh_2(diprop)_4]^{2+}$ cation is separated by calixarene anions (Fig. 4). The CH_2 groups of two *trans* diprop ligands form several H–π contacts with the benzene

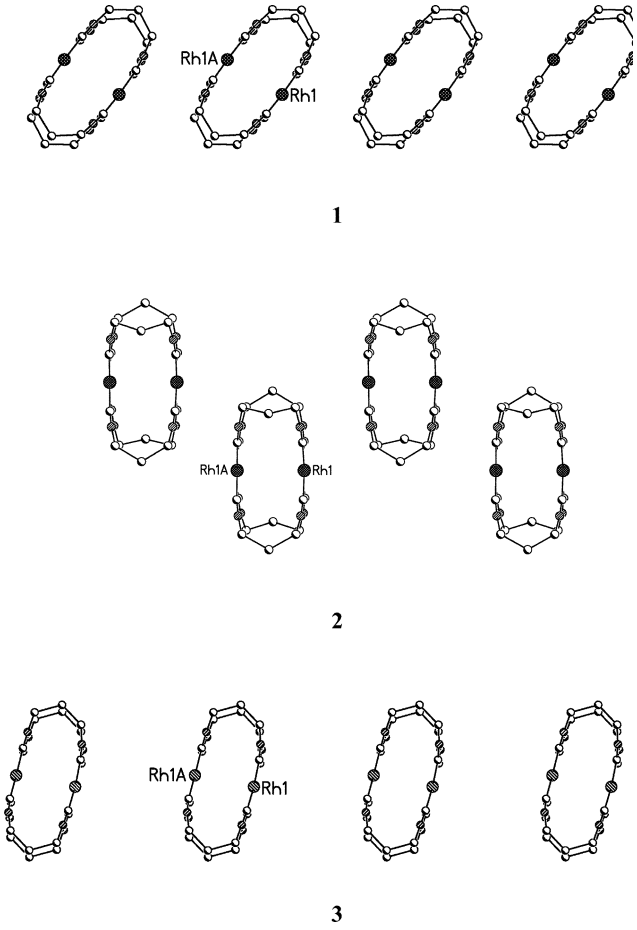

Fig. 3 Chains of $[Rh_2(diprop)_4]^{2+}$ cations in different solids: **1** ($[BPh_4]^-$), **2** ($[BPh_4]^-\cdot 1.0CH_3CN$) and **3** ($[BPh_4]^-\cdot 1.6C_6H_5CN 0.4C_6H_5Cl$). Chains are along the crystallographic *a*-axis in **1** and **3**, and along the *b*-axis in **2**.

rings of the calixarenes with distances of 2.53, 2.39, 2.36 Å (x, $1.5 - y$, $z - 0.5$) for one of the counterions, and 2.57 and 2.69 Å with the second counterion. Similarly, in **5** the $[Rh_2(dihex)_4]^{2+}$ cations are strictly monomeric.

However, with the larger calix[4]arene counterion (compound **6**) $[Rh_2(dihex)_4]^{2+}$ forms a dimeric aggregate in which the cation and inter-monomer Rh–Rh distances are at 3.207(2) and 3.202(2) Å equal within experimental error (Fig. 5). This dimerization affects the geometry around the Rh atoms. Rh2 is pyramidally distorted by a displacement of 0.08 Å from the plane through the four ligating C atoms towards the adjacent monomer, whereas Rh1, which is at the outside of the dimer, is tetrahedrally distorted. Similar to **4**, the cationic dimer forms H–π contacts with 2.66 and 2.88 Å ($0.5 - y$, $0.5 + x$, $z - 0.25$) distances to the benzene rings of adjacent calix[4]arene anions.

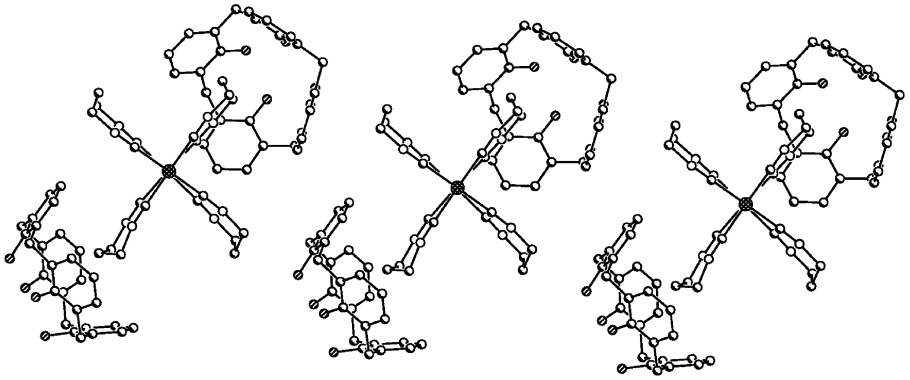

Fig. 4 Crystal packing diagram of **4** (calix[4]arenate).

Table 2 Solid state absorption and emission data

Cation	$[Rh_2(diprop)_4]^{2+}$			$[Rh_2(TMB)_4]^{2+}$		$[Rh_2(dihex)_4]^{2+}$		$[Rh_2(dimen)_4]^{2+}$		$[Rh_2(diprop)_4]^{2+}$	
Compound	**1** $[BPh_4]^-$	**3** $[BPh_4]^-$	**4** [Calix[4]-arenate]$^-$	PF_6^-,[7]	BPh_4^-,[25]	**5** $[PF_6]^-$	**6** [Calix[4]-arenate]$^-$	**7** $[PF_6]^-$	**8** [Calix[4]-arenate]$^-$	Eclipsed	Twisted
Experimental										Calculation[20]	
Rh–Rh/Å	3.296(1)	3.2397(6)	3.2262(5)	3.262	*b*	3.0988(7)	3.207(2)	4.5153(3)	4.033(1)	3.44	3.85
Twist angle (N≡)C–Rh–Rh–C(≡N)/°	≈1	≈2	≈6–9	≈30	*b*	≈54	≈56–58	≈0–2	≈0–3	2	27
UV-vis/nm Crystalline solid	570	*a*	570	*b*	533	525	*a*	427	433	674 (1.84 eV)	582 (2.13 eV)
DMSO solution	553	553	553	515	*b*	528	526	424	424		
Emission											
τ/μs (RT)	4.8	2.5	4.7	(0.03)[c]		No emission	No emission	No emission	*e*	n/a	
τ/μs (18 K)	8.7	6.6	6.2	(20.5, 77 K)[c]		13.2	18.0	10.9	7.5	n/a	
λ_{max}/nm (RT)	810	820	820	(≈780)[c]		No emission	No emission	No emission	*e*	n/a	
λ_{max}/nm (18 K)	830	845	845	(≈780, 77 K)[d]		786	785	600	685	n/a	

n/a–not applicable. [a] The amount of crystalline sample was not sufficient for the solid-state UV-vis spectra. [b] Data are not available, but expected to be similar for the two salts. [c] Solution or frozen matrix; V. M. Miskowski, S. F. Rice, H. B. Gray and S. J. Milder, *J. Phys. Chem.*, 1993, **97**, 4277–4283. [d] Frozen matrix; S. J. Milder, *Inorg. Chem.*, 1985, **24**, 3376–3378. [e] Emission is observed visually, but the lifetime is too short to be detected with our equipment.

Fig. 5 A view of compound **6** showing the dimeric $[Rh_2(dihex)_4]^{2+}$ cation surrounded by four calixarene anions.

Though polymerization of dinuclear rhodium compounds with Rh(I) and mixed Rh(I)Rh(II) oxidation states has been reported,[19–21] this is the first solid-state example of a dinuclear rhodium(I) compound forming dimers along the Rh–Rh axis. The Rh–Rh intermolecular interaction in the polymeric dirhodium(I) complex $Rh_2(\mu\text{-}O_2CCF_3)_2(CO)_4$ is similar to that observed here in terms of metal oxidation state and alignment of the neighbors along the Rh–Rh axis, but in $Rh_2(\mu\text{-}O_2CCF_3)_2(CO)_4$ the Rh–Rh distances are markedly different at 2.984 and 3.092 Å, respectively.[19]

Like the other two calix[4]arenate salts described in this study, the methyl group of the dimen ligand in **8** forms a 2.89 Å H–π contact with a benzene moiety of the calixarene counterion. In **8** the calixarene molecules form channels along the *a*-axis in which the dinuclear cations are located (Fig. 6).

Summary of previous spectroscopic studies

In solution (CH_3CN, 25 °C) the absorption spectrum of $[Rh_2(diprop)_4]^{2+}$ shows only one visible absorption band at 553 nm,[15] which has been assigned to the fully allowed $^1A_{1g} \rightarrow {}^1A_{2u}$ transition, corresponding to the promotion of a $4d_{z^2}$ σ*(HOMO) electron to the $5p_z\sigma$(LUMO) orbital.[15] The fluorescence lifetime of $[Rh_2(diprop)_4]^{2+}$ in acetonitrile solution at 25 °C is reported as <2 ns ($\lambda_{em} = 656$ nm), while the phosphorescence lifetime is ≈ 8.5 μs at 295 K ($\lambda_{em} = 830$ nm) and 16 μs at 77 K.[15,22] The 5 K single-crystal polarized absorption spectrum shows a vibronically structured band ($\lambda_{max} \approx 670$ nm),[23] identified as the weak singlet → triplet $\{^1A_{1g} \rightarrow E_u(^3A_{2u})\}$ transition.

For $[Rh_2(dimen)_4]^{2+}$ complexes the absorption corresponding to the singlet–singlet excitation is asymmetric, with a sharp maximum around 423 nm (PF_6^- salt) and a shoulder (≈480 nm) with a long-wavelength tail.[24] In contrast, the fluorescence (295 K) at 550 nm and phosphorescence emission bands (77 K) at 700 nm of the crystals are symmetric. The phosphorescence lifetime was found to be quite temperature dependent (τ_p = < 1 ns *vs.* 21 μs at 295 and 77 K, respectively).

UV-vis reflectance spectroscopy

The UV-Vis diffuse reflectance spectra of the solids (Fig. 7), are quite similar to the solution absorption spectra (Table 2). All compounds show only one visible band located between 427–578 nm (solid state) and 424–553 nm (solution), corresponding to the $^1A_{1g} \rightarrow {}^1A_{2u}$ transition.

Since the complexes with the more rigid cyclic dimen ligand have much larger Rh–Rh distances than those with the normal alkane bridges, the two groups will be discussed separately. The position of the absorption maxima are influenced by both the intermetallic distance and the twist angle. Contraction

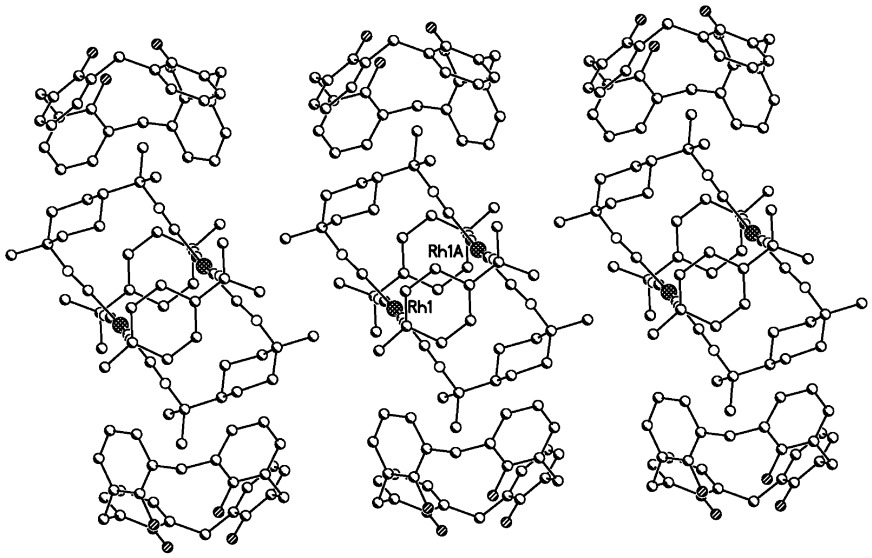

Fig. 6 Crystal packing diagram of **8**, $[Rh_2(dimen)_4][calix[4]arene - H]_2$.

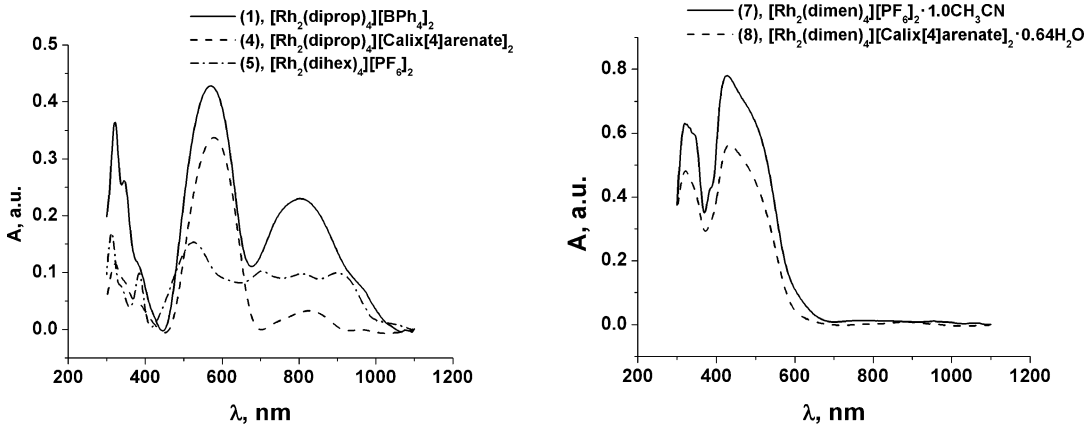

Fig. 7 UV-vis reflectance spectra for compounds **1**, **4**, **5**, **7** and **8**.

of the Rh–Rh distance increases the d_{z^2} Rh-atomic orbital overlap, thus destabilizing the anti-bonding HOMO orbital, which according to the calculations has a very large contribution from the d_{z^2} orbitals. This will reduce the HOMO and LUMO gap, in agreement with the results of our recent calculations on the $[Rh_2(diprop)_4]^{2+}$ cation.[12]

Comparison of the solid-state UV-vis data of **1**, **4**, **5**, with Rh–Rh distances in the 3.10–3.30 Å range (Table 2), shows that the large increase in the intra-ligand twist angle from very small to ≈54°, results in the $d\sigma^* \rightarrow p\sigma$ band shifting to higher energy (Fig. 8(a)). The twist-angle dependence was first noticed by Mann *et al.*[7,15a] in comparing the solution absorption spectra of $[Rh_2(diprop)_4]^{2+}$ and $[Rh_2(TM4\text{-}bridge)_4]^{2+}$ (TM4-bridge = 2.5-dimethyl-2,5-diisocyanohexane) (Table 2), which have similar Rh–Rh distances (3.19–3.26 Å range) but different rotameric conformations of the CNR groups. $[Rh_2(TM4\text{-}bridge)_4][BPh_4]_2$, with four C-atoms in the bridge shows the singlet-to-singlet band centered at 533 nm.[25] No crystal structure is available for this compound, though the hexafluorophosphate salt, which should be comparable, has an intermediate intra-ligand twist angle of about 30°.[7]

The blue shift that occurs on twisting is opposed by the red shift associated with Rh–Rh shortening. In the $[Rh_2(dimen)_4]^{2+}$ compounds **7** and **8**, the Rh–Rh distances are much larger and little twisting occurs. Accordingly, the $d\sigma^* \rightarrow p\sigma$ band is considerably blue shifted compared to its position in **1**, **4** and **5** (Table 2, Fig. 8(a)). The effect is most pronounced for **7**, which has the longest Rh–Rh distance. A similar behavior of the UV-vis solid-state spectra of the dimen compounds was observed earlier by Ekstrom *et al.*[5] in the tetrakis[3,5-bis(trifluoromethyl)phenyl]borate and tetraphenylborate salts.

As was noticed for the solution spectra of $[Rh_2(dimen)_4]^{2+}$ cation,[24] the UV-vis spectra of $[Rh_2(diprop)_4]^{2+}$ and $[Rh_2(dihex)_4]^{2+}$ in the visible region tend to be independent on the nature of the solvent and the anion. The similarity of the visible bands observed in the solution spectra of compounds **5** and **6** suggests that **6** becomes monomeric when dissolved.

Emission spectra and lifetimes

In the crystalline state diprop-bridged complexes **1**, **3** and **4** show strong near IR photoluminescence. Their phosphorescence emission is characterized by featureless spectra with the maxima positioned in the 810–820 and 830–845 nm range at room and low (18 K) temperatures, respectively (Table 2, Fig. 8(b)). At both temperatures, the emission maxima of compounds **3** and **4**, in which the Rh–Rh distances are shorter than in **1**, are red-shifted compared to **1**, indicating a smaller ^{3}ExS–GS energy gap in **3** and **4**. Thus, the shorter Rh–Rh distance, the smaller ^{3}ExS–GS energy difference, in a good agreement with the calculations on the $[Rh_2(diprop)_4]^{2+}$ molecule,[12] which show that the ^{3}ExS–GS energy gap of the $[Rh_2(diprop)_4]^{2+}$ cation narrows on shortening of the Rh–Rh distance.

According to the energy gap law,[26] the smaller ^{3}ExS–GS energy difference, the smaller the driving force for intersystem crossing and the shorter the excited state lifetime. This trend is confirmed by variation of the 18 K phosphorescence lifetimes of the three diprop complexes. Triplet state lifetimes were found

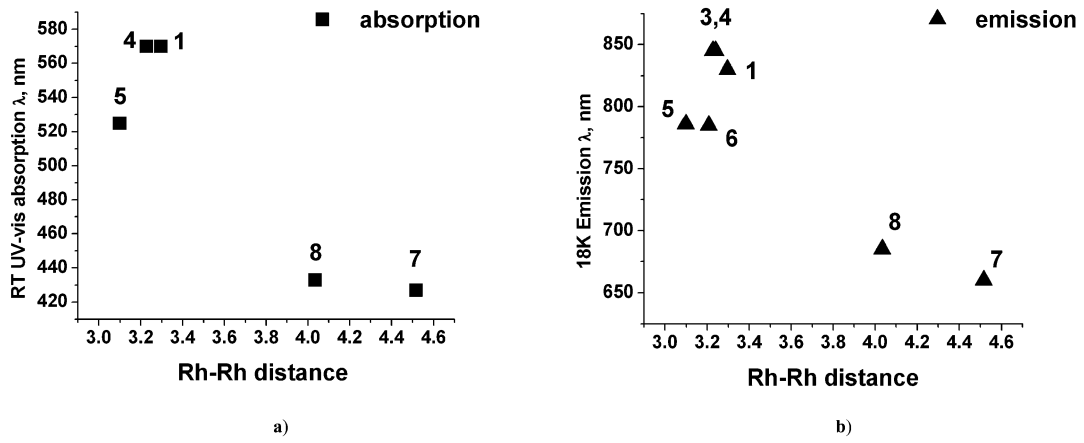

a) b)

Fig. 8 Correlation plots of UV-vis absorption (a, complexes **1**, **4**, **5**, **7** and **8**) and emission (b, complexes **1**, **3**–**8**) *vs.* Rh–Rh distance.

to be 8.7 μs for **1** (Rh–Rh ≈ 2.30 Å), but 6.6 and 6.2 μs for **3** and **4** (Rh–Rh ≈ 2.23 Å), respectively. Upon cooling the phosphorescence lifetime slightly increases. The largest change was found for **3**, its emission lifetime increasing by a factor of 2.5 on cooling to 18 K.

In contrast to the solid-state emission of the $[Rh_2(diprop)_4]^{2+}$ cation, the phosphorescence lifetime of $[Rh_2(dimen)_4]^{2+}$ in solution and rigid glasses was found to increase dramatically on cooling ($\tau_p < 1$ ns at 295 K *vs.* 21 μs at 77 K[24]). The same is true in the solid state for the two salts (**7** and **8**) examined here. At room temperature no luminescence with lifetimes above the sensitivity of our experimental equipment (≈ 100 ns) was detected. At 18 K compounds **7** and **8** exhibit intense orange photoluminescence with lifetimes of 10.9 μs for **7** and 7.5 μs for **8**. Like the absorption bands, the emission wavelengths are very much blue shifted compared with those of the other complexes surveyed here, in agreement with the much longer Rh–Rh distances (Fig. 8(b)). The emission maximum of compound **7** with the longer Rh–Rh distance and longer lifetime is centered at 660 nm, whereas the emission maximum of **8** with shorter Rh–Rh distance and shorter lifetime is red-shifted to 685 nm.

Only low-temperature (18 K) emission was detected with crystals of the dihex bridged complexes **5** and **6**. Their emission is weak, and in spite of the somewhat different Rh–Rh distances, the emission bands are both centered at around 785 nm (Table 2), although the lifetime of **5** (13.2 μs) is shorter than that of **6** (18 μs). The formation of cation dimers in the calixerate **6** may affect the photophysical properties.

In general, the triplet excited state lifetimes of the $[Rh_2(diprop)_4]^{2+}$ and $[Rh_2(dimen)_4]^{2+}$ cations in the solid state are shorter than the values reported for various solutions.[15,22,24] For example, the phosphorescence lifetime for $[Rh_2(diprop)_4]^{2+}$ in CH_3CN solution at room temperature is 8.5 μs, while it is 2.5–4.8 μs in the crystal at the same temperature. The lifetimes of $[Rh_2(dimen)_4]^{2+}$ at 18 K in **7** and **8** are at 10.9 and 7.5 μs, shorter than the 21 μs measured in the glass matrix 2-MeTHF–CH_3CN (3 : 1 v/v) at 77 K, suggesting increased intermolecular energy dissipation in the solid state.

Conclusions

The spectroscopy and crystallography of a series of salts of dirhodium(I) complexes with different bridging diisocyano ligands and different counterions have been investigated in the solid state. The studies demonstrate that Rh–Rh distance and the (N≡)C–Rh–Rh–C(≡N) twist angle vary considerably depending on the size and conformational rigidity of the ligand. The metal-to-metal distance is the shortest in $[Rh_2(dihex)_4]^{2+}$ in which ligand has the largest flexibility and longest in the $[Rh_2(dimen)_4]^{2+}$ cation with the more rigid dimen ligand. The Rh–Rh distance is sensitive to the crystalline environment, a difference as large as 0.5 Å is observed for the $[Rh_2(dimen)_4]^{2+}$ cation with different counterions, while an even shorter distance has been reported for the BPh_4 salt. For the complexes with normal alkane bridging ligands, the smallest (N≡)C–Rh–Rh–C(≡N) torsion angle is found for the $[Rh_2(diprop)_4]^{2+}$ cation, with its short diprop bridging ligand, whereas the largest twist angle occurs in $[Rh_2(dihex)_4]^{2+}$ in which the long dihex ligand allows considerable flexibility.

Solid-state UV-Vis diffuse reflectance spectra confirm that the red shift of the visible band for the binuclear Rh(I) compounds increases with contraction of the Rh–Rh distance and decreases with twist angle.

The first time-resolved X-ray diffraction experiments in this series, on $[Rh_2(dimen)_4](PF_6)_2$, have now been reported. They show a very large contraction of ≈0.85(5) Å of the Rh–Rh distance to 3.64(5) Å in the 10.9 μs lifetime triplet state.[10] Calculations on $[Rh_2(diprop)_4]^{2+}$ suggest that the shortening is very much a function of the ground state bond length: the calculated bond length shortens from 3.441 Å to 3.056 Å for the eclipsed ground state, but from 3.853 Å to 3.098 Å for the twisted state of the same complex, which corresponds to a somewhat higher minimum on the ground-state potential energy surface. Thus, the currently available information suggests the magnitude of the geometry change on excitation and the excited state Rh–Rh distance to be a function of the initial Rh–Rh distance. The factors that lead to the considerable variation in the ground state geometry also appear to affect the excited state structure.

Acknowledgements

We are grateful to Dr Milan Gembicky for his assistance with the synthesis of the 1,3-diisocyanopropane ligand. Financial support by the National Science Foundation (CHE9981864 and CHE0236317) and the Department of Energy (DE-FG02-02ER15372) is gratefully acknowledged.

References

1 N. S. Lewis, K. R. Mann, J. G. Gordon II and H. B. Gray, *J. Am. Chem. Soc.*, 1976, **98**, 7461–7463.
2 K. R. Mann, N. S. Lewis, V. M. Miskowski, D. K. Erwin, G. S. Hammond and H. B. Gray, *J. Am. Chem. Soc.*, 1977, **99**, 5525–5526.
3 I. S. Sigal, K. R. Mann and H. B. Gray, *J. Am. Chem. Soc.*, 1980, **102**, 7252.
4 P. D. Harvey, *Coord. Chem. Rev.*, 2001, **219–221**, 17–52.
5 C. L. Exstrom, D. Britton, K. R. Mann, M. G. Hill, V. M. Miskowski, W. P. Schaefer, H. B. Gray and W. M. Lamanna, *Inorg. Chem.*, 1996, **35**, 549–550 (See supplementary material).
6 K. R. Mann, *Cryst. Struct. Commun.*, 1981, **10**, 451–457.
7 K. R. Mann, J. A. Thich, R. A. Bell, C. L. Coyle and H. B. Gray, *Inorg. Chem.*, 1980, **19**, 2462–2468.

8 (*a*) W. K. Fullagar, G. Wu, C. Kim, L. Ribaud, G. Sagerman and P. Coppens, *J. Synchrotron Radiat.*, 2000, **7**(4), 229–235; (*b*) C. D. Kim, S. Pillet, G. Wu, W. K. Fullagar and P. Coppens, *Acta Crystallogr., Sect. A*, 2002, **58**, 133–137; (*c*) P. Coppens, I. I. Vorontsov, T. Graber, A. Yu. Kovalevsky, Y.-S. Chen, G. Wu, M. Gembicky and I. V. Novozhilova, *J. Am. Chem. Soc.*, 2004, **126**, 5980–5981; (*d*) I. Novozhilova, A. V. Volkov and P. Coppens, *J. Am. Chem. Soc.*, 2003, **125**, 1079–1087; (*e*) P. Coppens and I. Novozhilova, *Faraday Discuss.*, 2002, **122**, 1–11; (*f*) P. Coppens, *Chem. Commun.*, 2003, 1317–1320.
9 (*a*) S. Techert, F. Schotte and M. Wulff, *Phys. Rev. Lett.*, 2001, **86**, 2030–2033; (*b*) S. Techert and K. A. Zachariasen, *J. Am. Chem. Soc.*, 2004, **126**, 5593–5600.
10 P. Coppens, O. Gerlits, I. I. Vorontsov, A. Yu. Kovalevsky, Y.-S. Chen, T. Graber, M. Gembicky and I. V. Novozhilova, *Chem. Commun.*, 2004, 2144–2145.
11 P. Coppens, B. Ma, O. Gerlits, Y. Zhang and P. Kulshrestha, *CrystEngComm*, 2002, **4**, 302–309.
12 I. V. Novozhilova, A. V. Volkov and P. Coppens, *Inorg. Chem.*, 2004, **43**, 2299–2307.
13 W. P. Weber, G. W. Gokel and I. K. Ugi, *Angew. Chem., Int. Ed. Engl.*, 1972, **11**, 530–531.
14 J. M. Harrowfield, M. I. Ogden, W. R. Richmond, B. W. Skelton and A. H. White, *J. Chem. Soc., Perkin Trans. 2*, 1993, 2183–2190.
15 (*a*) K. R. Mann and H. B. Gray, *Adv. Chem. Ser.*, 1979, **173**, 225–235 (Inorg. Compd. Unusual Prop.-2); (*b*) V. M. Miskowski, G. L. Nobinger, D. S. Kliger, G. S. Hammond, N. S. Lewis, K. R. Mann and H. B. Gray, *J. Am. Chem. Soc.*, 1978, **100**, 485–488.
16 A. R. Rhodes and K. R. Mann, *Inorg. Chem.*, 1984, **23**, 2053–2058.
17 *SMART and SAINTPLUS - Area Detector Control and Integration Software, version 6.01*, Bruker AXS, Madison, WI, 1999.
18 *SHELXTL - An integrated system for Solving, Refining and Displaying Crystal Structures from Diffraction Data, version 5.10*, Bruker AXS, Madison, WI, USA, 1997.
19 F. A. Cotton, E. V. Dikarev and M. A. Petrukhina, *J. Chem. Soc., Dalton Trans.*, 2000, 4241–4243.
20 F. A. Cotton, E. V. Dikarev and M. A. Petrukhina, *J. Organomet. Chem.*, 2000, **596**, 130–135.
21 (*a*) C. Tejel, M. A. Ciriano, J. A. López, F. J. Lahoz and L. A. Oro, *Angew. Chem., Int. Ed.*, 1998, **37**(11), 1542–1545; (*b*) F. P. Pruchnik, P. Jakimowicz, Z. Ciunik, K. Stanislawek, L. A. Oro, C. Tejel and M. A. Ciriano, *Inorg. Chem. Commun.*, 2001, **4**, 19–22; (*c*) F. P. Pruchnik, P. Jakimowicz and Z. Ciunik, *Inorg. Chem. Commun.*, 2001, **4**, 726–729.
22 S. F. Rice, S. J. Milder, H. B. Gray, R. A. Goldbeck and D. S. Kliger, *Coord. Chem. Rev.*, 1982, **43**, 349–354.
23 S. F. Rice and H. B. Gray, *J. Am. Chem. Soc.*, 1981, **103**, 1593–1595.
24 V. M. Miskowski, S. F. Rice, H. B. Gray, R. F. Dallinger, S. J. Milder, M. G. Hill, C. L. Exstrom and K. R. Mann, *Inorg. Chem.*, 1994, **33**, 2799–2807.
25 S. F. Rice, V. M. Miskowski and H. B. Gray, *Inorg. Chem.*, 1988, **27**, 4704–4708.
26 N. J. Turro, *Modern Molecular Photochemistry*, University Science Books, Sausalito, CA, 1978.